Journal of Physiology (1993), **470**, *pp.* 295–311
With 9 figures
Printed in Great Britain

VOLTAGE-DEPENDENT BLOCK BY INTERNAL Ca^{2+} IONS OF INWARDLY RECTIFYING K^+ CHANNELS IN GUINEA-PIG VENTRICULAR CELLS

BY HIROKO MATSUDA AND JADER DOS SANTOS CRUZ*

From the Department of Physiology, Faculty of Medicine, Kyushu University, Fukuoka 812, Japan

(*Received 5 January 1993*)

SUMMARY

1. The block of the inwardly rectifying K^+ channel by intracellular Ca^{2+} was studied in guinea-pig ventricular cells.

2. Single-channel currents through the inwardly rectifying K^+ channel were recorded in the inside-out configuration at 150 mM external and internal K^+. Internal Ca^{2+}, at a concentration of 0·4–10 μM, induced subconductance levels with one-third and two-thirds of the unitary amplitude in the outward currents without affecting the inward currents.

3. Occupancy at each sublevel was estimated from the amplitude histogram which showed four equally spaced peaks in the presence of internal Ca^{2+}. At different degrees of blockade, the distribution of the current levels showed a reasonable agreement with the binomial theorem.

4. The outward mean open-channel currents were measured at different Ca^{2+} concentrations and voltages. The current–voltage relation rectified inwardly in the presence of internal Ca^{2+} in a concentration-dependent manner.

5. The outward mean open-channel currents were normalized to unitary amplitudes in the absence of Ca^{2+}. The normalized current–Ca^{2+} concentration curve was fitted by saturation kinetics with a Hill coefficient of 1 at each voltage. The voltage dependence of the dissociation constants gives the value for the fractional electrical distance of the Ca^{2+} binding site of 0·7.

6. The dwell times in each substrate were distributed exponentially. On the assumption that the inwardly rectifying K^+ channel of cardiac cells is composed of three identical conducting subunits and each subunit is blocked by Ca^{2+} independently, the blocking (μ) and unblocking (λ) rates were calculated. The value of μ increased with higher Ca^{2+} concentrations or larger depolarizations, while λ was independent of Ca^{2+} and decreased with larger depolarization.

7. It is thus concluded that internal Ca^{2+} produces a voltage-dependent block of the channel to cause inward rectification although the blocking effect is less potent than that of Mg^{2+}. The substate behaviour seen with internal Ca^{2+} supports the triple-barrelled structure of the cardiac inwardly rectifying K^+ channel.

* Present address: Departamento de Bioquimica, ICB, Universidade Federal de Minas Gerais, Belo Horizonte, Brazil.

MS 1997

INTRODUCTION

Most cardiac K^+ channels show inward rectification, permitting a greater entry of K^+ under hyperpolarization than exits under depolarization. This behaviour plays an important role in maintaining the long-lasting action potential characteristic of cardiac cells. The mechanism by which such rectification might occur has remained a puzzle for close to 40 years since it was first reported in the resting K^+ conductance of skeletal muscles (Katz, 1949). Recently, however, evidence has been accumulating from several cardiac K^+ channels that voltage-dependent block by internal Mg^{2+} and Na^+ causes the inward rectification; in the inwardly rectifying K^+ channel (Matsuda, Saigusa & Irisawa, 1987; Vandenberg, 1987; Matsuda, 1993); in the adenosine 5′-triphosphate (ATP)-regulated K^+ channel (Kakei, Noma & Shibasaki, 1985; Findlay, 1987; Horie, Irisawa & Noma, 1987); in the Na^+-activated K^+ channel (Wang, Kimitsuki & Noma, 1991) and in the muscarinic receptor-operated K^+ channel (Horie & Irisawa, 1987, 1989).

Ca^{2+} exists inside the cells under physiological conditions as well as Mg^{2+} and Na^+. According to an earlier report by Mazzanti & DiFrancesco (1989), internal Ca^{2+} at submicromolar levels induces outward current sublevels with a quarter and three-quarters of the unit amplitude. Inward rectification was ascribed to favouring the channel closing by internal Ca^{2+} rather than to a blockade of the channel.

We have observed sublevels with one-third and two-thirds of the unit amplitude in the block by internal Mg^{2+} (Matsuda, 1988, 1991) and by external Cs^+ and Rb^+ (Matsuda, Matsuura & Noma, 1989) and have proposed that the cardiac inwardly rectifying K^+ channel consists of three identical conducting units. Thus the report that internal Ca^{2+} induced sublevels with a quarter and three-quarters of the unit amplitude interested us very much and tempted us to re-examine the effects of internal Ca^{2+}. We have now obtained results differing from those of previous studies: sublevels induced in the outward current by internal Ca^{2+} have amplitudes of one-third and two-thirds of the unitary amplitude and internal Ca^{2+} acts as an open-channel blocker to prevent the channel from closing.

METHODS

Preparations. Guinea-pigs were anaesthetized with intraperitoneal injections of sodium pentobarbitone (30 mg kg^{-1}) and the chest was opened under artificial respiration. The ascending aorta was cannulated *in situ* and the heart was dissected out. The blood was washed out by coronary perfusion with Tyrode solution equilibrated with 100% O_2. The composition of the main solutions is listed in Table 1. After the heart was perfused with about 50 ml of Ca^{2+}-free Tyrode solution, a Ca^{2+}-free Tyrode solution containing 3·5 mg dl^{-1} collagenase (Yakult) was perfused for about 10 min. Thereafter, collagenase was washed out with 100 ml of a high-K^+, low-Cl^- solution containing (mM): KCl, 30; glutamic acid, 70; KH_2PO_4, 10; $MgCl_2$, 1; taurine, 20; Hepes, 10; glucose, 10; and ethyleneglycol-bis-(β-aminoethylether)*N,N,N′,N′*-tetracetic acid (EGTA), 0·3; pH was adjusted to 7·3 with KOH. The temperature of all perfusates was kept at 36–37 °C during coronary perfusion, and the hydrostatic pressure for perfusion was approximately 65 cmH_2O. Finally, the ventricles were cut and chopped with scissors. Gentle agitation of the chunks released the cells into the high-K^+, low-Cl^- solution. The cells were filtered through a 150 μm mesh net and centrifuged at 800 r.p.m. for 4 min. The cell pellet was resuspended in modified Eagle's medium (Flow Laboratories, Irvine, Scotland) and then kept at room temperature, 22–24 °C.

Recording techniques. Recordings of single-channel currents were performed using a heat-polished patch electrode (Hamill, Marty, Neher, Sakmann & Sigworth, 1981). Pipettes were made from

capillaries of hard borosilicate glass (Pyrex) and were coated near their tips with silicone to reduce electrical capacitance. The electrode resistance ranged between 7 and 15 MΩ when filled with a 150 mM KCl pipette solution.

The current records illustrated in this paper were obtained from inside-out patches. After the giga-seal was attained in Tyrode solution, nominally Ca^{2+}-free Tyrode solution and then 150 mM K^+, divalent cation-free solution were perfused. The patch was excised in the latter solution by

TABLE 1. Composition of solutions (mM)

Bathing solution

	NaCl	NaH_2PO_4	KCl	$CaCl_2$	$MgCl_2$	Hepes	Glucose	V_j (mV)
Tyrode solution	140	0·33	5·4	1·8	0·5	5	5·5	0

	Potassium aspartate	KCl	KH_2PO_4	$CaCl_2$	EGTA	K_2ATP	Hepes	V_j (mV)
150 mM K^+, Ca^{2+} free	60	65	1	0	5	3	5	−9·5
150 mM K^+, Ca^{2+} test	55	65	1	4·31–5·06	5	3	5	−9·5

Pipette solution

	KCl	$CaCl_2$	Hepes	V_j (mV)
150 mM K^+	150	1	5	−2·0

The pH of the solutions was adjusted to 7·4 with KOH or NaOH (Tyrode solution). The K^+ concentration after titration was approximately 155 mM in internal solution and 152 mM in 150 mM K^+ pipette solution.

V_j was the liquid junction potential between the solution and the Tyrode solution. (The sign was positive when the Tyrode solution side was negative.)

moving the pipette away from the cell. ATP at a concentration of 3 mM suppressed the ATP-regulated K^+ channel. Thus the channel observed constantly under this condition was the inwardly rectifying K^+ channel responsible for the resting conductance. The channel activity in the inside-out patches was maintained for as long as 20–30 min. The free Ca^{2+} concentration of the bathing solution was buffered using EGTA. The calculation of the free Ca^{2+} concentration was done by a computer program (Fabiato & Fabiato, 1979; Tsien & Rink, 1980) using the dissociation constants (Martell & Smith, 1974) corrected for temperature and ionic strength (Harrison & Bers, 1989). The temperature of the solution in the chamber was kept at 24–26 °C.

Recordings were made with an EPC-7 patch clamp amplifier (List electronic, Darmstadt, Germany). A steady potential was applied to the inside of the electrode to set the holding potential of the membrane patch, and outward currents were elicited by depolarizing steps of 130 ms every 1 s. The membrane potentials are expressed in the conventional way, inside relative to outside, and outward currents are ascribed a positive sign. The membrane potentials were corrected for the liquid junction potential at the tip of the patch pipette in Tyrode solution and also for that at the tip of the indifferent reference electrode filled with Tyrode solution in the bathing solution.

Data analysis. Data were recorded on a digital audio tape using a PCM data recorder (TEAC, RD-101T) and stored for subsequent computer analysis (NEC, PC-98 XL). The currents were filtered using a four-pole low-pass Bessel filter (NF, FV-665) with a −3 dB corner frequency of 1·2 kHz and sampled every 0·2 ms, unless otherwise indicated. Capacitive and leakage currents were removed by the transient cancellation facility of the amplifier and by subtracting from each trace the average of the current traces without events. The mean open-channel currents were calculated from twenty to forty frames as follows. A threshold was set just above the zero-current level and data points below the threshold were averaged. The difference between each data point lying above the threshold and the averaged baseline was calculated, and the differences were integrated. The resulting integrated value was then divided by the duration of the channel opening. Current amplitudes were measured by forming histograms of the baseline and open-level data points and then these histograms were fitted with Gaussian curves using a least-squares algorithm to find the area under each curve, its mean and variance. To measure the mean dwell time in each substate, the current records with single-channel activity, which were filtered at 2 kHz and digitized at 5 kHz, were reconstructed by setting a threshold level at around half of the open level

of the subunits for discrimination of open and blocked states of subunits. The dwell-time histogram in each substate was formed from reconstructed traces and then fitted with an exponential function using a least-squares algorithm. The average results throughout this paper are given as mean ± S.D.

RESULTS

Substate conductance in the presence of internal Ca^{2+}

Outward single-channel currents through the inwardly rectifying K^+ channel are not recorded in the cell-attached configuration (Sakmann & Trube, 1984), but appear in response to voltage steps or voltage ramps to levels more positive than the equilibrium potential for K^+ (E_K) when the internal surface of the cell is exposed to divalent cation-free K^+ solution. The current–voltage (I–V) relation for the single channel is ohmic, and inward rectification is restored when Mg^{2+}, Ca^{2+} or Na^+ is added to the internal bathing solution (Matsuda *et al.* 1987; Vandenberg, 1987; Matsuda, 1988, 1991, 1993; Mazzanti & DiFrancesco, 1989).

Figure 1 shows the inward currents recorded in a steady-state condition (left panel) and outward currents induced by voltage steps to levels more positive than E_K (right panel) in the presence of 3·7 μM internal Ca^{2+}. E_K, predicted from a 150 mM external and internal K^+ concentration, is 0 mV. Current records obtained at a driving force of nearly the same amplitude but of opposite direction are arranged in the same row. Inward currents show long-lasting openings characteristic of the inwardly rectifying K^+ channel. Internal Ca^{2+} affects neither the current amplitude nor the channel kinetics of the inward current (see below). In contrast to this, the outward open channel showed, as in the Mg^{2+} block, two discrete subconductance levels equally spaced and fluctuating between four levels including these intermediate levels in addition to the fully open channel current and the zero-current levels. As voltage is made increasingly positive, the probability of observing the lower levels progressively increases, while that of observing the higher levels decreases.

Figure 2*A* shows the outward current at different Ca^{2+} concentrations during a clamp pulse to +69 mV from a holding potential of −48 mV. In the absence of internal Ca^{2+}, the outward open channel stayed fully open most of the time. In the presence of Ca^{2+}, frequent transitions were observed between the sublevels. As the Ca^{2+} concentration was increased, the current was more likely to be at lower levels and the fluctuations became more rapid.

The appearance when the channel is open, of four equally spaced conductance levels (including the zero-current level) suggests that the cardiac inwardly rectifying K^+ channel consists of three identical conducting units that usually are regulated by a common gate to act as a single channel and that Ca^{2+} may enter and plug up each subunit at positive potentials. Sublevels with one-third or two-thirds of the unit amplitude are also induced in the outward current by the internal application of Mg^{2+} (Matsuda, 1988, 1991) and in the inward current by the external application of Cs^+ or Rb^+, although, unlike Mg^{2+} and Ca^{2+} block, not in all channels (Matsuda *et al.* 1989). Our previous studies showed that the open-state occupancies of each current level are in reasonable agreement with the binomial theorem, suggesting that each subunit is blocked by the blocking ions independently (Matsuda, 1988; Matsuda *et al.* 1989).

To know whether the open-state occupancies of each current level (the fraction of the total time for which the current stayed at each level) conform to a binomial

distribution in the block by Ca^{2+}, histograms of current amplitude were constructed (Fig. 2*B*). For this purpose, zero-current periods longer than 10 ms have been attributed to the closed state of the channel and excluded from the analysis in the presence of Ca^{2+}. The histogram without internal Ca^{2+} is well fitted by the sum of two

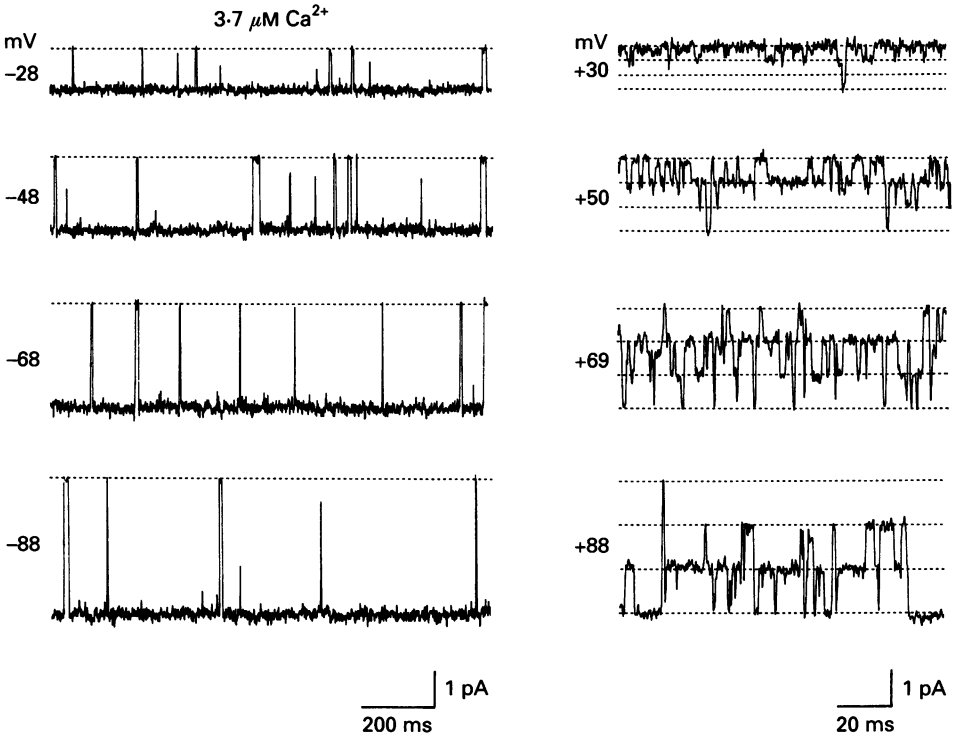

Fig. 1. Single-channel currents recorded from an inwardly rectifying K^+ channel in the inside-out configuration in the presence of 3·7 μM internal Ca^{2+}. The numbers to the left of each current trace refer to holding potential (left panel), or the potential levels during the depolarizing steps from −48 mV (right panel). Currents in the left panel were filtered at 1 kHz and sampled every 1 ms. The dotted lines indicate the zero-current level (left panel) and, from the top, the current levels of fully open, two-thirds, one-third and zero (right panel) (It is the same in Fig. 2.).

Gaussian distributions. The distribution of non-zero current amplitudes with Ca^{2+} showed two other peaks of intermediate size in addition to the largest peak. It is evident in the figure that internal Ca^{2+} affects the distribution of the current levels during the open state.

The amplitude histograms were fitted with Gaussian curves and the occupancies at current levels of zero (P_0), one-third (P_1), two-thirds (P_2) and fully open (P_3) were calculated from the area under each curve. The distributions of the sublevels obtained at different Ca^{2+} concentrations (0·4–3·7 μM) and voltages in three experiments are summarized in Fig. 3, where the occupancies of each level are plotted against the open probability of subunits (p) together with theoretical curves of P_0, P_1, P_2 and P_3. (The equations to represent occupancies at current levels are given in figure legend.) The value of p was calculated by dividing the mean open-channel current by

the unitary amplitude without Ca^{2+}. The occupancies at each current level are, on the whole, in agreement with the binomial theorem. However, some deviations from the theoretical curves were observed, and will be dealt with in more detail in the Discussion.

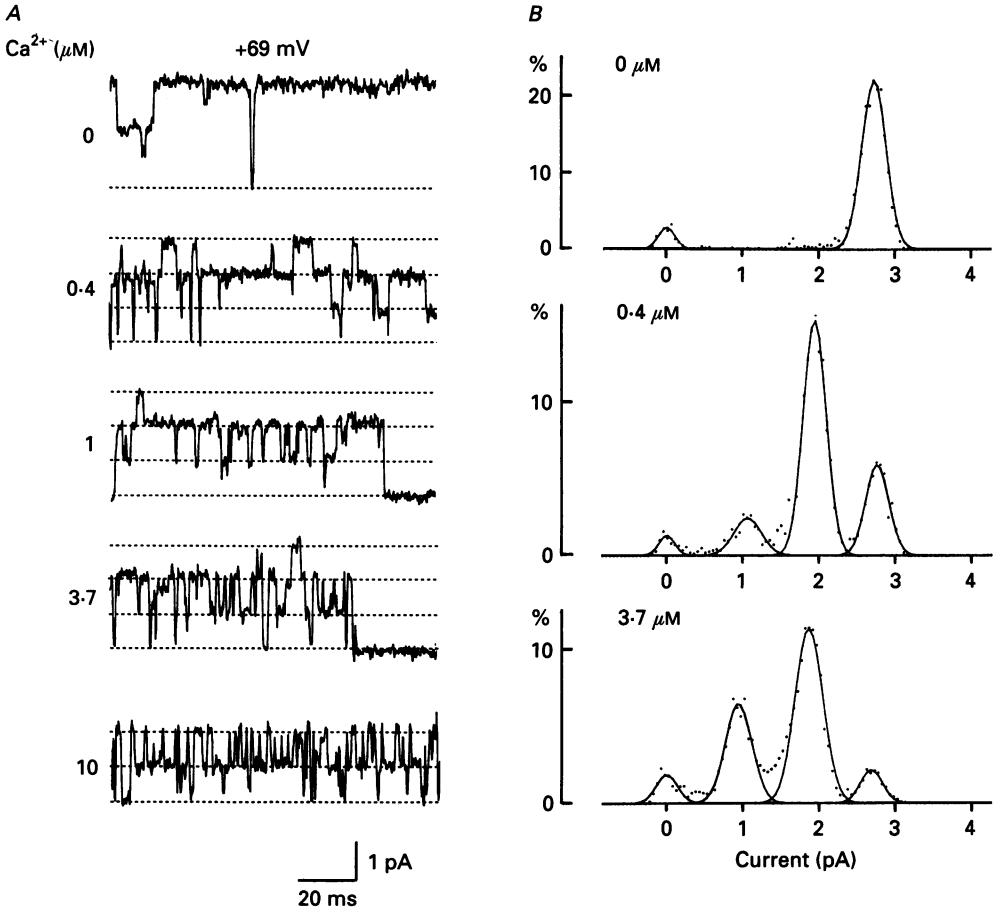

Fig. 2. *A*, effect of internal Ca^{2+} on the outward single-channel current. After recording the control trace while perfusing the inside-out patch membrane with Ca^{2+}-free solution, the Ca^{2+} concentration of the perfusing solution was increased progressively. Depolarizing step to +69 mV from −48 mV. The same patch as in Fig. 1. *B*, histograms of current amplitude with 0, 0·4 and 3·7 μM Ca^{2+} from the same patch as in *A*. The curve is the sum of two (without Ca^{2+}) or four (with Ca^{2+}) Gaussian distributions fitted by a least-squares method. The parameters (area, mean, standard deviation) were: 0·077, 0, 0·11; 0·876, 2·66, 0·16 without Ca^{2+}: 0·035, 0, 0·10; 0·112, 1·05, 0·18; 0·583, 1·91, 0·15; 0·225, 2·71, 0·15 with 0·4 μM Ca^{2+}: 0·066, 0, 0·14; 0·283, 0·92, 0·17; 0·521, 1·83, 0·18; 0·078, 2·62, 0·14 with 3·7 μM Ca^{2+}.

Quantification of the Ca^{2+} block

To quantify the blocking effect of Ca^{2+} and compare it with that of Mg^{2+}, outward mean open-channel currents were calculated from twenty to forty frames in the presence of Ca^{2+}. Unitary amplitudes of outward currents without Ca^{2+} and inward

currents were estimated from the amplitude histograms. Figure 4 shows the *I–V* relations at different Ca^{2+} concentrations (0–10 μM). In the presence of internal Ca^{2+}, the chord conductance was decreased at potentials positive to E_K. Depression of the outward current was increased with increasing Ca^{2+} concentration and depolar-

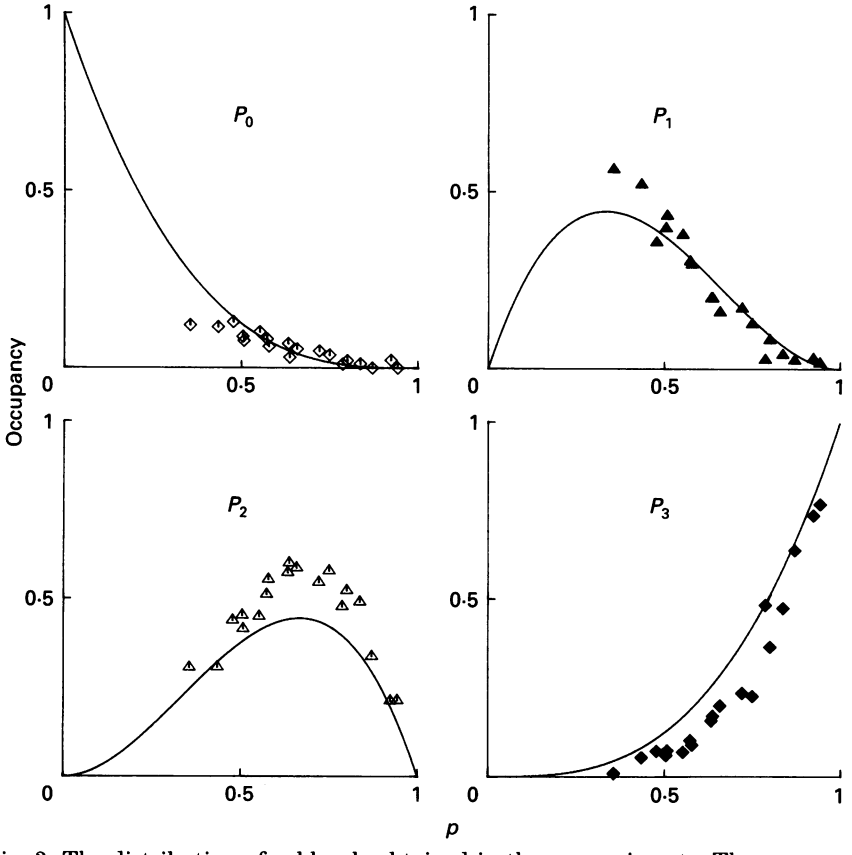

Fig. 3. The distribution of sublevels obtained in three experiments. The occupancies at different Ca^{2+} concentrations and voltages were plotted against the open probability of subunits (p). The theoretical curves in each panel were drawn from the following equations: $P_0 = (1-p)^3$, $P_1 = 3p(1-p)^2$, $P_2 = 3p^2(1-p)$ and $P_3 = p^3$.

ization. On the other hand, the unitary amplitudes of inward currents were not affected by 10 μM internal Ca^{2+}.

The mean open-channel current was normalized to the unitary amplitude in the absence of Ca^{2+} and plotted against the Ca^{2+} concentration (Fig. 5). The results at +30 and +50 mV fit well with the concentration–effect curves predicted by assuming one-to-one binding of Ca^{2+} to a site, while some deviation from the theoretical curves was observed at more positive potentials. Dissociation constants were calculated by fitting the data to saturation kinetics with a Hill coefficient of 1.

In a semilogarithmic plot of dissociation constant *versus* membrane potential, data points can be fitted by a straight regression line, indicating that the dissociation

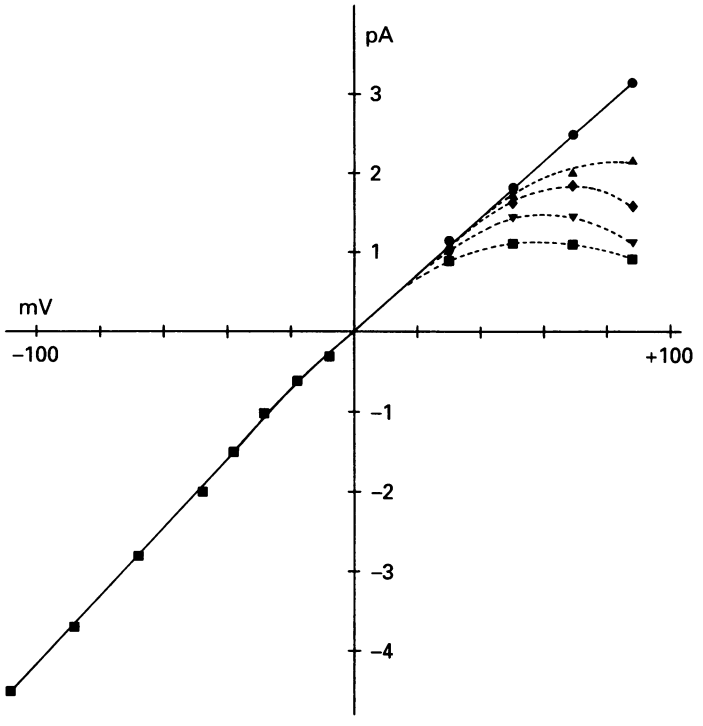

Fig. 4. Current–voltage relationship obtained at a Ca^{2+} concentration of 0 (●), 0·4 (■), 1 (◆), 3·7 (▼) and 10 (■) μM. Data points represent unitary amplitudes of outward currents without Ca^{2+} and inward currents or outward mean open-channel currents with Ca^{2+}. Unitary amplitudes of inward currents without Ca^{2+} are almost identical to those with Ca^{2+} and are omitted in the figure. In this patch the slope conductance was increased slightly at potentials more negative than −20 mV.

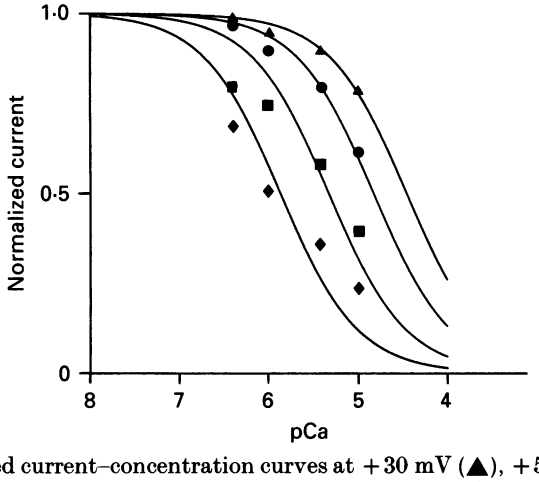

Fig. 5. Normalized current–concentration curves at +30 mV (▲), +50 mV (●), +69 mV (■) and +88 mV (◆). Data points represent the mean value of three to five experiments. Deviations from the mean value were 0·01–0·05. Each curve was fitted by saturation kinetics with a Hill coefficient of 1. Dissociation constants are 35·2 μM at +30 mV, 14·9 μM at +50 mV, 4·7 μM at +69 mV and 1·3 μM at +88 mV.

constant decreases exponentially as the membrane potential is increased (Fig. 6). The dissociation constant at a membrane potential of V, $K_D(V)$, is described as:

$$K_D(V) = K_D(0)\exp(-z\delta VF/RT),$$

where z is the valency of the blocking ion, and δ is the fractional electrical distance between the internal mouth of the aqueous pore and the Ca^{2+} binding site (Woodhull,

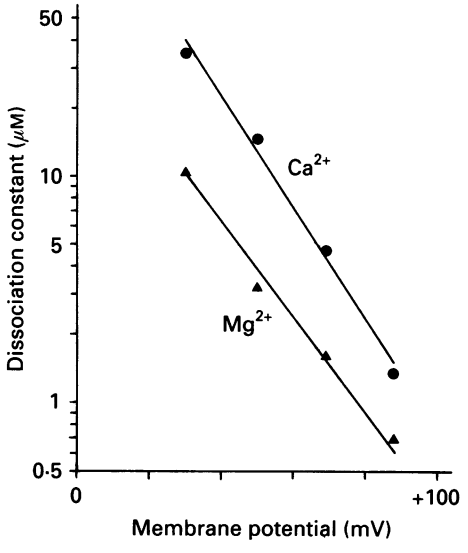

Fig. 6. Dependence of the dissociation constant of divalent blockers on membrane potential. On this semilogarithmic plot, data are fitted by a straight line. The slope of the regression line gave the fractional electrical distance of the Ca^{2+} binding site, $\delta = 0{\cdot}7$. The dissociation constants for Mg^{2+} obtained in a previous work (Matsuda, 1991) are shown for comparison ($\delta = 0{\cdot}6$).

1973). F, R and T have their usual meaning. The slope of the regression line gave a value of 0·7 for δ. Dissociation constants obtained for internal Mg^{2+} in the same experimental conditions (Matsuda, 1991) are also shown in the figure for comparison. The dissociation constants for Mg^{2+} are smaller than those for Ca^{2+} but the slope is similar ($\delta = 0{\cdot}6$), indicating the same location for the site with a higher affinity.

Kinetics of Ca^{2+} block

The kinetic properties of blockage associated with substate behaviour were studied based on the binomial scheme (Matsuda, 1988; Matsuda *et al.* 1989). If the block of each subunit is described as:

$$O \underset{\lambda}{\overset{\mu}{\rightleftharpoons}} B,$$

where O and B are the open and blocked states of each subunit, λ is the first-order unblocking rate and μ the blocking rate given by the product of the second-order rate

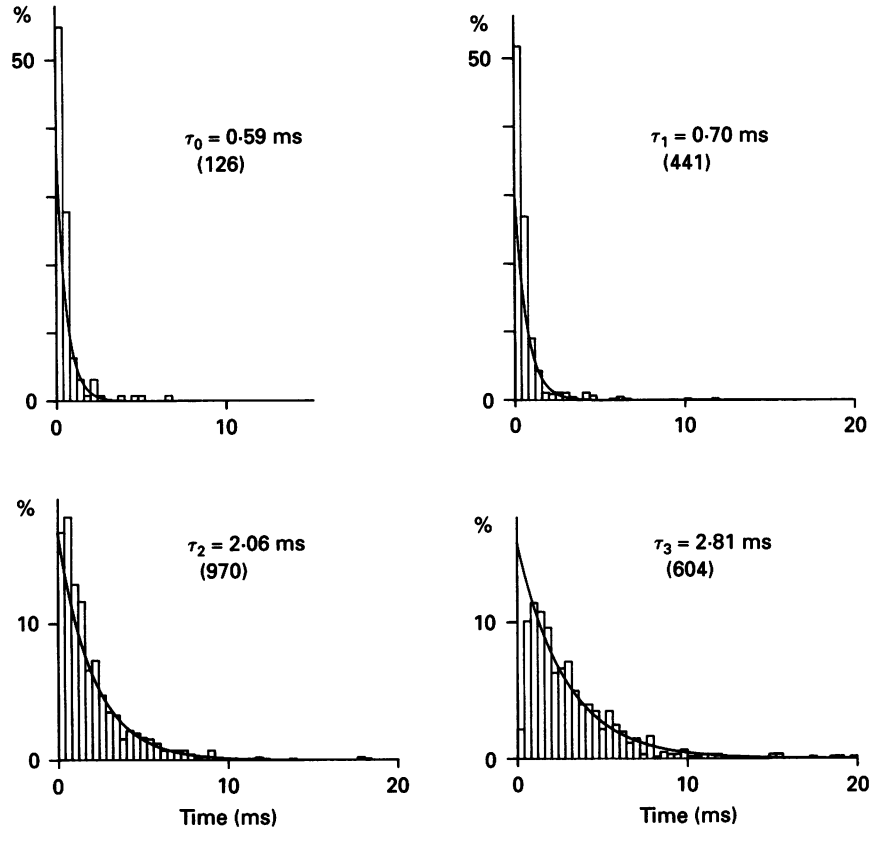

Fig. 7. Dwell-time histograms in each substate at +50 mV with 1 μM Ca^{2+}. The histograms were formed in 0·4 ms bins and fitted with a single-exponential function with the time constant indicated. The numbers of events are shown in parentheses. The first bin was omitted for fitting the histogram in O_3 (lower right panel).

constant and the concentration of blocker, the open-state probability of the subunits, p, is expressed as $\lambda/(\lambda+\mu)$ and transitions between substates during the open state of the channel can be described as:

$$O_3 \underset{\lambda}{\overset{3\mu}{\rightleftharpoons}} O_2 \underset{2\lambda}{\overset{2\mu}{\rightleftharpoons}} O_1 \underset{3\lambda}{\overset{\mu}{\rightleftharpoons}} O_0,$$

where O_0, O_1, O_2 and O_3 are the substates in which all, two, one and none of the three subunits are blocked, respectively. In this scheme,

$$1/\tau_0 = 3\lambda,$$
$$1/\tau_1 = 2\lambda+\mu,$$
$$1/\tau_2 = \lambda+2\mu,$$
$$1/\tau_3 = 3\mu,$$

where τ_0, τ_1, τ_2 and τ_3 represent the mean lifetimes in 0_0, 0_1, 0_2 and 0_3, respectively.

Dwell-time histograms in each substate were compiled from the reconstructed traces. Figure 7 gives an example obtained with 1 μM Ca^{2+} at +50 mV. The dwell-time histograms could be fitted by single-exponential functions with the time constants indicated. λ and μ were calculated from τ_0 and τ_3, respectively. Table 2 lists measurements at different voltages and the Ca^{2+} concentrations in the experiment

TABLE 2. Kinetic analysis of substates

Ca^{2+} (μM)	Voltage (mV)	τ_0 (ms)	τ_1 (ms)	τ_2 (ms)	τ_3 (ms)	p	μ (s^{-1})	λ (s^{-1})
0·4	+50	0·59	0·62 (0·83)	2·01 (1·42)	4·78	0·91 (0·89)	69·7	565·0
	+69	1·04	1·23 (1·35)	3·17 (1·93)	3·38	0·75 (0·76)	98·6	320·5
	+88	1·23	1·58 (1.47)	2·35 (1·81)	2·38	0·62 (0·66)	140·1	271·0
1·0	+50	0·59	0·70 (0·80)	2·06 (1·25)	2·81	0·83 (0·83)	118·6	565·0
	+69	0·80	1·00 (0·99)	2·00 (1·29)	1·85	0·67 (0·70)	180·2	416·7
	+88	1·17	1·38 (1·20)	1·56 (1·23)	1·27	0·50 (0·52)	262·5	284·9
3·7	+50	0·53	0·57 (0·71)	2·06 (1·07)	2·18	0·80 (0·80)	152·9	628·9
	+69	0·88	0·93 (0·97)	1·55 (1·07)	1·20	0·58 (0·58)	277·8	378·8
	+88	1·30	1·46 (1·05)	1·20 (0·88)	0·76	0·36 (0·37)	438·6	256·4

μ and λ were calculated from τ_3 and τ_0. The theoretical values of τ_1, τ_2 and p are listed in parentheses.

shown in Fig. 7. Theoretical values predicted from the blocking and unblocking rates are shown in parentheses.

The blocking and unblocking rates listed in Table 2 are plotted on a semilogarithmic scale against the membrane potential in Fig. 8. The blocking rate μ increases exponentially with more positive potentials, while the unblocking rate λ decreases. μ increases with increasing Ca^{2+} but the linearly proportional relation between μ and the Ca^{2+} concentration was not observed. λ is almost independent of the Ca^{2+} concentration.

Effects of internal Ca^{2+} on the channel kinetics

The results presented so far have described the voltage-dependent block of the inwardly rectifying K^+ channel by internal Ca^{2+}. Previous studies have shown that a voltage-dependent gating mechanism does exist independently of the block by internal cations (Matsuda *et al.* 1987; Matsuda, 1988). We thus studied whether Ca^{2+} can modulate gating kinetics. In the open cell-attached configuration (Matsuda, 1988), outward openings appeared some 2–5 min after rupturing the cell membrane

and the open times of the channel in the outward direction increased with time during perfusion of the divalent cation-free K^+ solution. On the other hand, outward openings of long duration were observed immediately after excision of the patch membrane in the inside-out configuration. Such a difference suggests that a soluble

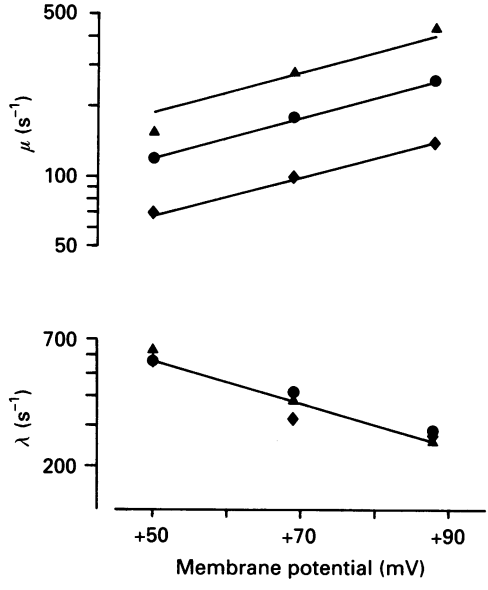

Fig. 8. Voltage dependence of blocking (μ) and unblocking (λ) rates. μ and λ calculated for the experiment shown in Fig. 7 (Table 2) were plotted on a semilogarithmic scale against membrane potential. ◆, 0·4 μM; ●, 1 μM; ▲, 3·7 μM.

component associated with channel closing may be taken away more drastically in the inside-out configuration than in the open cell-attached configuration. However, the intrinsic gating was still preserved in the inside-out configuration and the average outward current in the absence of internal Ca^{2+} decayed with a time course which could be fitted with a single-exponential function (Fig. 9*A*).

Calcium ions at a concentration of 1 μM slowed the decay of the average current and increased the current amplitude at the end of a 130 ms depolarizing pulse. These effects can be explained by assuming that the channel cannot close when any subunit of the channel is blocked by Ca^{2+} (i.e. the closed state is assumed to be to the left of the O_3 state in the sequential schemes) and also that the block rate is much larger than the closing rate. Indeed the block rate ($3\mu = 355{\cdot}8\ s^{-1}$: Table 2) is twentyfold larger than the closing rate ($< 20\ s^{-1}$; the reciprocal of the time constant for relaxation of the average current in the absence of Ca^{2+} gives the sum of the opening and closing rates). Because the channel in substates O_1 and O_2 allows current of one-third and two-thirds of the unit amplitude, a partial block of the channel produces a larger steady-state current than without Ca^{2+}. Similar results were also obtained in the block by internal Mg^{2+} (Matsuda, 1988).

As mentioned before, internal Ca^{2+} does not affect the gating kinetics in the inward current. The open-time histograms in the absence and presence of 1 μM Ca^{2+} were

fitted with a single-exponential function having nearly the same time constant (Fig. 9*B*). About 90% of the closed times were fitted by a single-exponential function, whose time constant was also not affected by internal Ca^{2+}: 4·43 ms without Ca^{2+} and 4·22 ms with Ca^{2+} (not shown).

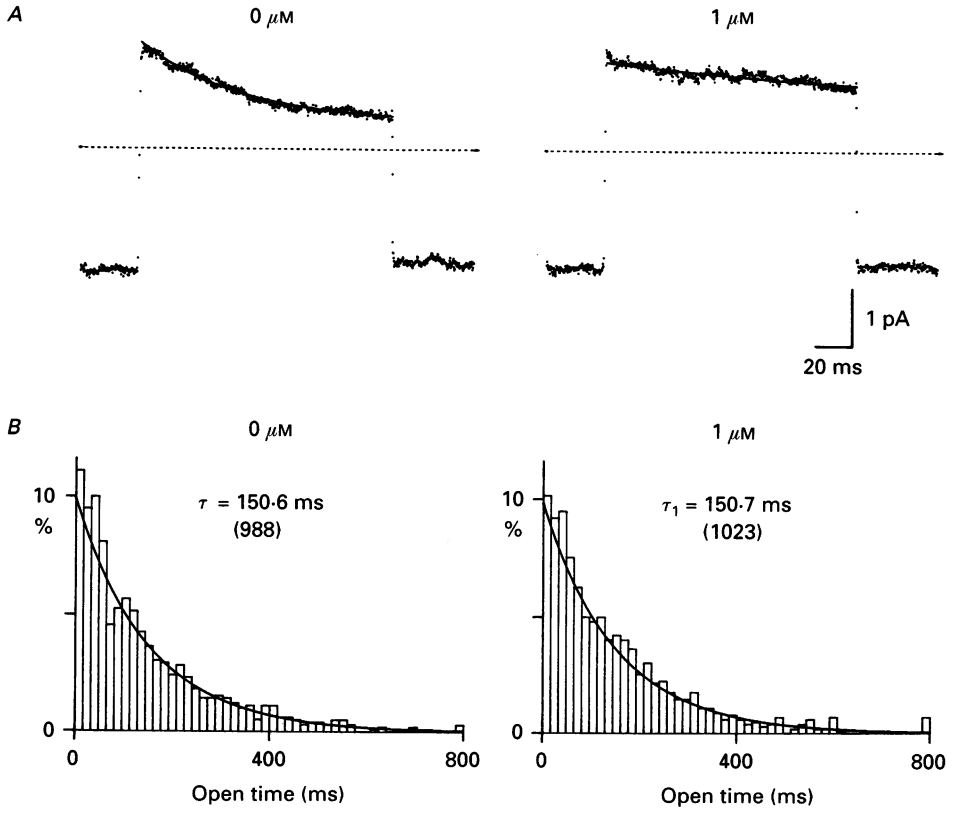

Fig. 9. *A*, slowing of the decay of the average outward current by internal Ca^{2+}. The membrane potential was held at −48 mV and depolarized to +50 mV. The average current was obtained from 89 (0 μM) and 101 (1 μM) frames and is plotted by points. The dotted line indicates the zero-current level. The time constant of the exponential decay (shown by the continuous line) was 50·0 ms (0 μM) and 179·6 ms (1 μM). Note that the current amplitude at the end of the 130 ms pulse was increased by Ca^{2+}. A rapid decay seen at the onset of the pulse in the presence of Ca^{2+} may represent the process of the block. *B*, the open-time histograms of the inward current in the absence and presence of 1 μM Ca^{2+}. Open and closed times were measured using a cursor set midway between the open and closed levels. Holding potential, −48 mV; filter, 1 kHz; sample rate, 5 kHz. The same patch as shown in Table 2.

DISCUSSION

In this work, the effects of internal Ca^{2+} ions on the inwardly rectifying K^+ channel were studied. Internal Ca^{2+} at a micromolar level blocks the channel in a voltage-dependent way and induces sublevels with one-third and two-thirds of the unit amplitude in the outward current. Previous studies reported that internal Ca^{2+}

induced sublevels of one-quarter and three-quarters of the unit amplitude (Mazzanti & DiFrancesco, 1989). The cause of the different results in the same preparation and recording technique (the inside-out configuration) is still unknown.

The frequent transitions of the open-channel current between four equally spaced conductance levels including the zero-current level were also observed during the block by internal Mg^{2+} (Matsuda, 1988, 1991) and external Cs^+ or Rb^+ (Matsuda *et al.* 1989). The substate behaviour can be explained by assuming that the cardiac inwardly rectifying K^+ channel consists of three identical conducting units which usually function co-operatively to form a single channel and that blocking ions enter and plug up each subunit.

Another possible mechanism that may induce sublevels is the binding of the blocking ions to a site on the channel protein leading to different conductive states in a single-barrel channel. In this case the binding of different kinds of ions should cause the same conformational changes of the channel to induce sublevels with the same amplitudes. Besides, considering electrostatic repulsion, it is unlikely that more than two blocking ions can bind to one site. If we assume that one blocking ion binds to a site, complicated conformation changes should be involved for one blocking ion to produce discrete decreases of the single-channel conductance to zero, one-third and two-thirds of the unitary conductance.

The open-state occupancies at each current level approximately followed a binomial distribution. However, some deviations from the theoretical curves were observed. In terms of the binomial model, five measurable quantities, τ_0, τ_1, τ_2, τ_3 and p, yield calculations of two rates, λ and μ. This allows the validity of the binomial model to be tested by calculating the blocking and unblocking rates from some of the measurements and comparing the other experimental values with the values calculated using these rates. In this work τ_3 and τ_0 were used to estimate μ and λ. The calculated open probability and time constant, τ_1, showed a close agreement with the observed values, while the theoretical value of τ_2 was smaller than the observed value (Table 2). These results imply some co-operative interactions between the conducting units during the Ca^{2+} block.

Therefore, we re-evaluated the transition rates using the mean dwell times and open-state occupancies in the substates in the linear sequential model, which is now rewritten as:

$$O_3 \underset{\lambda_3}{\overset{\mu_3}{\rightleftharpoons}} O_2 \underset{\lambda_2}{\overset{\mu_2}{\rightleftharpoons}} O_1 \underset{\lambda_1}{\overset{\mu_1}{\rightleftharpoons}} O_0.$$

In the steady state,

$$P_1 \mu_1 = P_0 \lambda_1,$$
$$P_2 \mu_2 = P_1 \lambda_2,$$
$$P_3 \mu_3 = P_2 \lambda_3.$$

The mean dwell times in the substates are given by:

$$1/\tau_0 = \lambda_1,$$
$$1/\tau_1 = \lambda_2 + \mu_1,$$
$$1/\tau_2 = \lambda_3 + \mu_2,$$
$$1/\tau_3 = \mu_3.$$

For example, the transition rates obtained at +69 mV with 3·7 μM Ca^{2+} were: λ_3, 135·4 s^{-1} (compare with the value based on the binomial theorem $\lambda = 378{\cdot}8\ s^{-1}$); μ_2, 509·8 s^{-1} ($2\mu = 555{\cdot}5\ s^{-1}$); λ_2, 840·3 s^{-1} ($2\lambda = 757{\cdot}6\ s^{-1}$); μ_1, 235·0 s^{-1} ($\mu = 277{\cdot}8\ s^{-1}$). The value of λ_3 is smaller than that predicted from the binomial theorem in all cases ($0{\cdot}42 \pm 0{\cdot}15$; $n = 9$), while μ_1 shows wide variations between cases (0·39–4·18; $2{\cdot}03 \pm 1{\cdot}40$). The values of μ_2 and λ_2 are relatively close to the theoretical values ($0{\cdot}88 \pm 0{\cdot}22$ and $0{\cdot}96 \pm 0{\cdot}14$, respectively). It has been suggested that some mechanism may exist which retains Ca^{2+} in the conducting unit longer than expected from the binomial model when the other two units are free. In the Mg^{2+} block, where μ and λ were determined from τ_1, τ_2 and p, the duration of zero-current states (τ_0) was shorter than expected from the binomial model (Matsuda, 1988). This indicates that the exit rate of Mg^{2+} from the conducting unit is increased when all units are occupied by Mg^{2+} and can be explained by assuming electrostatic repulsion between Mg^{2+} ions belonging to neighbouring units. Although some interactions between the conducting units are suggested, we consider the binomial model approximately describes the block of the cardiac inwardly rectifying K^+ channel with the sublevels.

Since the blocking rate μ is equal to the second-order rate constant ($M^{-1}\ s^{-1}$) multiplied by the concentration of the blocking ion, μ would be expected to be directly proportional to the Ca^{2+} concentration. However, this was not the case (Table 2). We measured the free Ca^{2+} concentration with a Ca^{2+}-sensitive electrode (Model 93-20, Orion Research, Boston, MA, USA) and excluded the possibility that inaccuracy in buffering the Ca^{2+} concentration might result in a deviation from the linearly proportional relation. The blocking rate was almost proportional to the Mg^{2+} concentration in the Mg^{2+} block (Matsuda, 1988) and at present we cannot find out the reason for the sublinear dependence of μ on the Ca^{2+} concentration. The blocking rate constant calculated from μ at 3·7 μM Ca^{2+} is $4{\cdot}1 \times 10^7\ M^{-1}\ s^{-1}$ at +50 mV, $7{\cdot}5 \times 10^7\ M^{-1}\ s^{-1}$ at +69 mV and $11{\cdot}9 \times 10^7\ M^{-1}\ s^{-1}$ at +88 mV. We consider these values to be the most reliable, which give nearly the same dissociation constant as that obtained from the normalized current–Ca^{2+} concentration curve.

The voltage dependence of the dissociation constant gave a value for the fractional electrical distance of the Ca^{2+} binding site of 0·7. A value for the fractional electrical distance between the inner mouth of the pore and the peak of the energy barrier and the distance between the energy barrier and the binding site of the blocking ion is given by the voltage dependence of μ and λ, respectively (Woodhull, 1973). They were both 0·26 and resulted in a value of 0·52 for the Ca^{2+} binding site. Values of 0·57 and 0·5 were obtained for the Mg^{2+} binding site (Matsuda, 1991) and the Na^+ binding site (Matsuda, 1993), respectively. The sites for internal blocking ions to bind seem to be located near each other.

Mazzanti & DiFrancesco (1989) suggested that internal Ca^{2+} favours channel closing at voltages positive to E_K and induces rectification. We observed, however, an opposite effect, slower decay of the average outward current and a larger late current indicating that the channel is stuck in the open state by the presence of Ca^{2+} in the channel. We thus consider that internal Ca^{2+} causes the inward rectification through blockade of the channel. The physiological concentration of internal Na^+ is about 10 mM (e.g. Blatter & McGuigan, 1991) and higher than that of internal Mg^{2+} or Ca^{2+}. The dissociation constants for Na^+ are, however, several times larger than

the physiological Na^+ concentration, suggesting that the contribution of internal Na^+ to the inward rectification is not significant (Matsuda, 1993). As shown in Fig. 6, the dissociation constants for Mg^{2+} are smaller than those for Ca^{2+}. Furthermore, the physiological concentration of internal Mg^{2+} in the heart muscle lies between 0·5 and 1 mM (McGuigan, Blatter & Buri, 1991), while the Ca^{2+} concentration is around 1 μM at maximum (Wendt-Gallitelli & Isenberg, 1991; Hongo, Tanaka & Kurihara, 1993). Although the actual local concentration of Ca^{2+} in the subsarcolemmal space might be higher than the bulk concentration, it can be concluded that Mg^{2+} plays a major role in producing inward rectification under physiological conditions.

Mazzanti & DeFelice (1990) recorded unitary currents through the inwardly rectifying K^+ channel in the cell-attached configuration in spontaneously beating chick ventricular cells while recording action potentials. The whole-cell electrode contained about 2 mM Mg^{2+} but outward unitary currents ascribed to the inwardly rectifying K^+ channel were recorded during the plateau phase. From the observation that the average outward currents were increased by removing Ca^{2+} from the pipette solution for single-channel current recordings, the authors have suggested the possibility that Ca^{2+} flows into the cell through the Ca^{2+} channel to affect the inwardly rectifying K^+ channel in the vicinity. In guinea-pig ventricular cells, outward single-channel currents through the inwardly rectifying K^+ channel were not recorded in the cell-attached configuration even using Ca^{2+}-free, EGTA-containing pipette solution (H. Matsuda, unpublished observation).

We thank Professor A. Noma for his comments on the manuscript, Dr T. Shioya for providing the computer program for data acquisition and Dr B. T. Quinn for reading the manuscript. This work was supported by a grant from the Ministry of Education, Science and Culture of Japan. J. S. Cruz was supported by a scholarship from CNPq (Conselho Nacional de Desenvolvimento científico e Tecnológico), Brazil.

REFERENCES

BLATTER, L. A. & MCGUIGAN, J. A. S. (1991). Intracellular pH regulation in ferret ventricular muscle. The role of Na–H exchange and the influence of metabolic substrates. *Circulation Research* **68**, 150–161.

FABIATO, A. & FABIATO, F. (1979). Calculator programs for computing the composition of the solutions containing multiple metals and ligands used for experiments in skinned muscle cells. *Journal de Physiologie* **75**, 463–505.

FINDLAY, I. (1987). ATP-sensitive K^+ channels in rat ventricular myocytes are blocked and inactivated by internal divalent cations. *Pflügers Archiv* **410**, 313–320.

HAMILL, O. P., MARTY, A., NEHER, E., SAKMANN, B. & SIGWORTH, F. J. (1981). Improved patch-clamp techniques for high-resolution current recording from cells and cell-free membrane patches. *Pflügers Archiv* **391**, 85–100.

HARRISON, S. M. & BERS, D. M. (1989). Correction of proton and Ca association constants of EGTA for temperature and ionic strength. *American Journal of Physiology* **256**, C1250–1256.

HONGO, K., TANAKA, E. & KURIHARA, S. (1993). Alterations in contractile properties and Ca^{2+} transients by β- and muscarinic receptor stimulation in ferret myocardium. *Journal of Physiology* **461**, 167–184.

HORIE, M. & IRISAWA, H. (1987). Rectification of muscarinic K^+ current by magnesium ion in guinea pig atrial cells. *American Journal of Physiology* **253**, H210–214.

HORIE, M. & IRISAWA, H. (1989). Dual effects of intracellular magnesium on muscarinic potassium channel current in single guinea-pig atrial cells. *Journal of Physiology* **408**, 313–332.

HORIE, M., IRISAWA, H. & NOMA, A. (1987). Voltage-dependent magnesium block of adenosine-triphosphate-sensitive potassium channel in guinea-pig ventricular cells. *Journal of Physiology* **387**, 251–272.

KAKEI, M., NOMA, A. & SHIBASAKI, T. (1985). Properties of adenosine-triphosphate-regulated potassium channels in guinea-pig ventricular cells. *Journal of Physiology* **363**, 441–462.

KATZ, B. (1949). Les constantes électriques de la membrane du muscle. *Archives des Sciences Physiologiques* **3**, 285–300.

MCGUIGAN, J. A. S., BLATTER, L. A. & BURI, A. (1991). Use of ion selective microelectrodes to measure intracellular free Mg^{2+}. In *Mg^{2+} and Excitable Membranes*, ed. STRATA, P. & CARBONE, E., pp. 1–19. Springer–Verlag, Berlin, Heidelberg.

MARTELL, A. E. & SMITH, R. M. (1974). *Critical Stability Constants*, vol. 1, *Amino Acids*. Plenum Press, New York.

MATSUDA, H. (1988). Open-state substructure of inwardly rectifying potassium channels revealed by magnesium block in guinea-pig heart cells. *Journal of Physiology* **397**, 237–258.

MATSUDA, H. (1991). Effects of external and internal K^+ ions on magnesium block of inwardly rectifying K^+ channels in guinea-pig heart cells. *Journal of Physiology* **435**, 83–99.

MATSUDA, H. (1993). Effects of internal and external Na^+ ions on inwardly rectifying K^+ channels in guinea-pig ventricular cells. *Journal of Physiology* **460**, 311–326.

MATSUDA, H., MATSUURA, H. & NOMA, A. (1989). Triple-barrel structure of inwardly rectifying K^+ channels revealed by Cs^+ and Rb^+ block in guinea-pig heart cells. *Journal of Physiology* **413**, 139–157.

MATSUDA, H., SAIGUSA, A. & IRISAWA, H. (1987). Ohmic conductance through the inwardly rectifying K channel and blocking by internal Mg^{2+}. *Nature* **325**, 156–159.

MAZZANTI, M. & DEFELICE, L. J. (1990). Ca modulates outward current through I_{K1} channels. *Journal of Membrane Biology* **116**, 41–45.

MAZZANTI, M. & DIFRANCESCO, D. (1989). Intracellular Ca modulates K-inward rectification in cardiac myocytes. *Pflügers Archiv* **413**, 322–324.

SAKMANN, B. & TRUBE, G. (1984). Conductance properties of single inwardly rectifying potassium channels in ventricular cells from guinea-pig heart. *Journal of Physiology* **347**, 641–657.

TSIEN, R. Y. & RINK, T. J. (1980). Neutral carrier ion-selective microelectrodes for measurement of intracellular free calcium. *Biochimica et Biophysica Acta* **599**, 623–638.

VANDENBERG, C. A. (1987). Inward rectification of a potassium channel in cardiac ventricular cells depends on internal magnesium ions. *Proceedings of the National Academy of Sciences of the USA* **84**, 2560–2564.

WANG, Z., KIMITSUKI, T. & NOMA, A. (1991). Conductance properties of the Na^+-activated K^+ channel in guinea-pig ventricular cells. *Journal of Physiology* **433**, 241–257.

WENDT-GALLITELLI, M. F. & ISENBERG, G. (1991). Total and free myoplasmic calcium during a contraction cycle: X-ray microanalysis in guinea-pig ventricular myocytes. *Journal of Physiology* **435**, 349–372.

WOODHULL, A. M. (1973). Ionic blockage of sodium channels in nerve. *Journal of General Physiology* **61**, 687–708.